SCIENCE AND TECHNOLOGY ORGANIZATION
CENTRE FOR MARITIME RESEARCH AND EXPERIMENTATION

Reprint Series **CMRE-PR-2019-094**

Maritime surveillance with multiple over-the-horizon HFSW radars: an overview of recent experimentation

Paolo Braca, Salvatore Maresca, Raffaele Grasso,
Karna Bryan, Jochen Horstmann

June 2019

Originally published in:

IEEE Aerospace and Electronic Systems Magazine, volume 30, issue 12, December 2015, pp. 4-18, doi: 10.1109/MAES.2015.150004

About CMRE

The Centre for Maritime Research and Experimentation (CMRE) is a world-class NATO scientific research and experimentation facility located in La Spezia, Italy.

The CMRE was established by the North Atlantic Council on 1 July 2012 as part of the NATO Science & Technology Organization. The CMRE and its predecessors have served NATO for over 50 years as the SACLANT Anti-Submarine Warfare Centre, SACLANT Undersea Research Centre, NATO Undersea Research Centre (NURC) and now as part of the Science & Technology Organization.

CMRE conducts state-of-the-art scientific research and experimentation ranging from concept development to prototype demonstration in an operational environment and has produced leaders in ocean science, modelling and simulation, acoustics and other disciplines, as well as producing critical results and understanding that have been built into the operational concepts of NATO and the nations.

CMRE conducts hands-on scientific and engineering research for the direct benefit of its NATO Customers. It operates two research vessels that enable science and technology solutions to be explored and exploited at sea. The largest of these vessels, the NRV Alliance, is a global class vessel that is acoustically extremely quiet.

CMRE is a leading example of enabling nations to work more effectively and efficiently together by prioritizing national needs, focusing on research and technology challenges, both in and out of the maritime environment, through the collective Power of its world-class scientists, engineers, and specialized laboratories in collaboration with the many partners in and out of the scientific domain.

NOTE: The CMRE Reprint series reprints papers and articles published by CMRE authors in the open literature as an effort to widely disseminate CMRE products. Users are encouraged to cite the original article where possible.

Maritime Surveillance with Multiple Over-the-Horizon HFSW Radars: An Overview of Recent Experimentation

Paolo Braca *Raffaele Grasso* *Jochen Horstmann*
Salvatore Maresca *Karna Bryan*
NATO STO Centre for Maritime Research & Experimentation
La Spezia, Italy

Helmholtz-Zentrum Geesthacht, Germany

INTRODUCTION

Maritime surveillance (MS) is an important domain for many national and international institutions, agencies, and bodies. In this context, the MS initiatives are aimed to enhance search and rescue operations, provide effective response to accidents and disasters, monitor fisheries, prevent pollution and support law enforcement and national defence. This means that it is of vital importance to generate real-time wide-area maritime operational pictures. However, many are the issues at stake. For instance, deriving mission planning tools with multiple stakeholders and achieving coverage with a wide choice of platforms (coastal, airborne and satellite) are just some of the problems. In addition, it could be required to correlate results with intelligence data and to integrate radar systems with the automatic identification system (AIS) and vessel traffic services (VTS). Other issues could be providing navigational risk detection to support operators, as well as improving resource allocation for greater efficiency and cost savings. Having access to other services, such as weather and environment information, could be precious for route planning. Additionally, timely and robust ways of sharing data and information between the authorities need to be developed with the objective of maximizing the sustainable use of oceans and seas, while enhancing the knowledge and innovation potential in maritime affairs.

In support to the MS framework comes the rapid development of information and communications technology, with the increasing availability of surveillance sensors, data stored in databases, networked system solutions and robust signal processing techniques. However, in order to provide comprehensive operational pictures, this data needs to be condensed in the right way, in order not to overwhelm the human decision-making process. As a matter of fact, the concept of data fusion (DF) has been introduced and, over the years, several solutions have been proposed to face the many operational challenges [1]–[6]. In this context, asset allocation, route planning and anomaly detection tasks are just some of the possible applications.

In the MS domain, it is easy to understand that long-range cost-effective sensors operating continuous-time may play a key role. Among these, in recent times low-power oceanographic high-frequency surface-wave (HFSW) radar systems have started to raise significant attention. Although their principal task is ocean remote sensing, they have been demonstrated to be very promising for ship detection and tracking purposes at over-the-horizon (OTH) distances. Multiple HFSW radar sensors, if used in combination with other types of sensors, such as the navigation reports from the AIS system, can grant continuous-time coverage of large sea areas and, thus, act as cost-effective early-warning sensors. In this paper, an experimental multitarget tracking data fusion (MTT-DF) system for ship traffic monitoring is described [7] based on multiple Wellen radar (WERA) systems [8]. Specifically for a single operating WERA system, a preliminary MTT system was proposed in [9] and then a more sophisticated one in [10].

This paper briefly explores the HFSW radar technology in general, and WERA in more detail. Then it describes the MTT-DF network architecture developed at Science and Technology Organization (STO) Centre for Maritime Research and Experimentation (CMRE) and discusses its capabilities in two real study cases: the first in the Ligurian Sea, Mediterranean (see Figure 1(a)) [11]–[13], and a second in the German Bight, North Sea (see Figure 1(b) and Figure 2) [14], [15]. In both cases, the main task of the HFSW radars is to estimate sea surface currents. In the second study case, the data recorded by the single stations are sent directly to the Centre's Data Base (DB) and then processed in real-time. The historical information about ship traffic can be exploited not only for assessing system performance, but also in the field of knowledge-based (KB) tracking, for improving system capabilities. In this sense, simulation results are presented and discussed. Finally, a tool developed at STO CMRE, the so-called maritime situational awareness (MSA) viewer, allows displaying from the operator's point of view the maritime picture of the surveyed area.

THE HFSW RADAR SYSTEM

HFSW radars exploit the HF band, i.e., the 3–30 MHz frequency interval, with wavelengths between 100 and 10 m, respectively. In this frequency range, vertically polarized electromagnetic

Authors' address: NATO STO Centre for Maritime Research & Experimentation, Research Dept.,Viale San Bartolomeo 400, La Spezia, Italy 19126. E-mail: (paolo.braca@cmre.nato.int).
Manuscript received January 12, 2015, revised June 5, 2015, and ready for publication July 27, 2015.
DOI No. 10.1109/MAES.2015.150004.
Review handled by W. Blair.
0885/8985/15/$26.00

waves also have the ability to propagate as ground waves, along a conductive surface, such as the ocean due to its salinity. The ability to look over the horizon, together with the low-power requirements of each site (i.e. about 30–50 W on average, exploiting continuous-wave instead of pulsed signals), have made HFSW radars ideal for long-range ocean remote sensing applications [16], e.g. surface currents [17], wind extraction, wave retrieval [18] and lately the application for tsunami early-warning detection [19]. An interesting walk-through of HFSW radars can be found in [20] and references therein.

THE SYSTEM SETUP

The design of WERA involves a combination of hardware and software solutions, in order to grant good dynamic range and modularity [16]. A typical WERA system installation along the coast is shown in Figure 3. In order to maximize the coupling with the sea surface, these systems should be deployed close to the shore. The transmitter (Tx) and receiver (Rx) are made by $\lambda_0/4$ monopole arrays, where λ_0 is the electromagnetic carrier wavelength. The Tx has a rectangular arrangement, while the Rx has a linear arrangement, with 12 or 16 array elements. The two separate locations for the Tx and Rx allow for simultaneous transmit and receive operations. Depending on the desired operation, the system requires hundreds of meters of available space along a straight line. The angle w.r.t. north of the Rx array installation is denoted with ϕ_0 and measured clockwise. The final field of view of the radar is about 120° around the broadside direction, i.e. $\phi_0 - 90°$. WERA operates at 35 W on average and uses linear frequency modulated continuous wave (LFMCW) chirps, with a repetition interval of T_c. In the following, the chirp bandwidth will be denoted with B and the corresponding range resolution with ΔR.

THE SYSTEM COMPONENTS AND PREPROCESSING SCHEME

The most crucial component of an FMCW radar is the chirp generator. The direct digital synthesizer (DDS) allows generating a

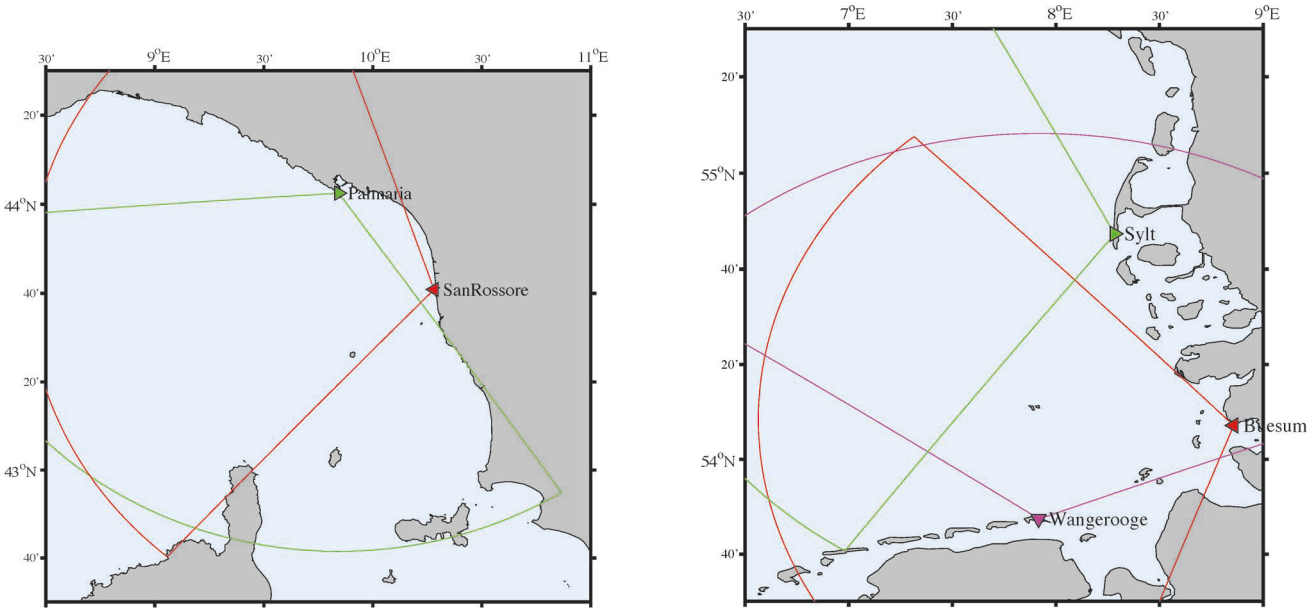

Figure 1.
Setup of the HFSW radars in the Ligurian Sea (a) and German Bight (b) and their areas of coverage. Subfigure (a): Palmaria (green), San Rossore (red). Subfigure (b): Sylt (green), Büsum (red), and Wangerooge (magenta).

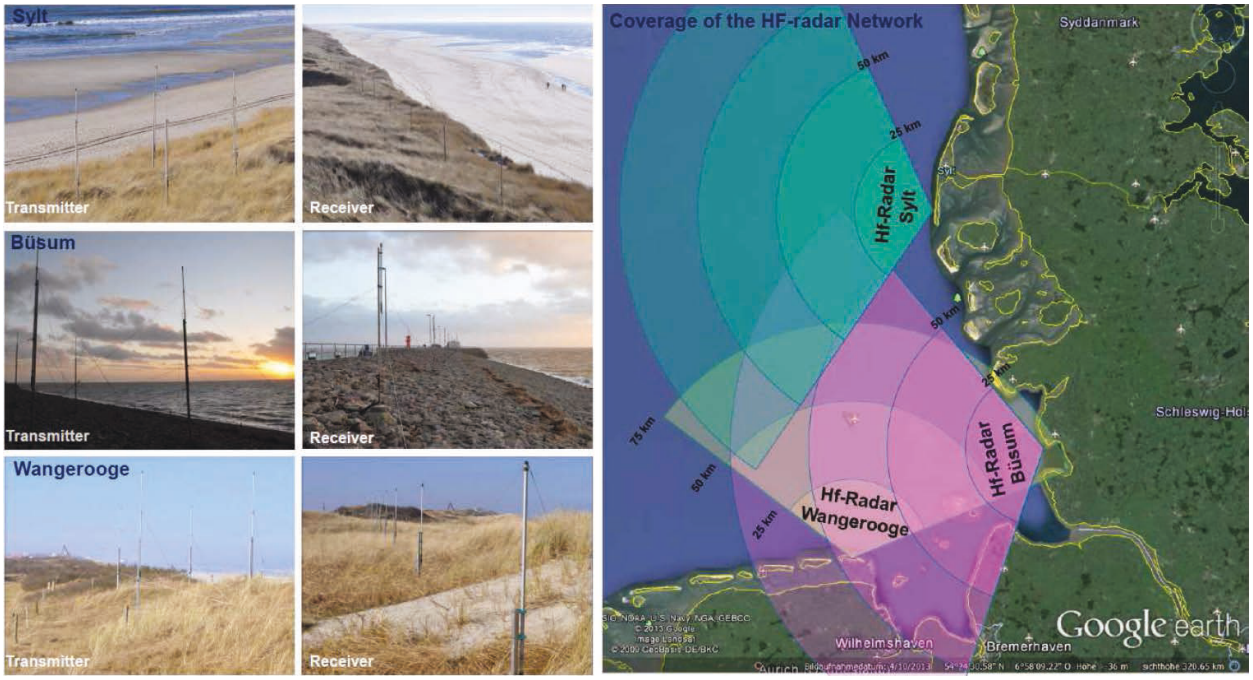

Figure 2.
Images of Sylt, Büsum, and Wangerooge transmitters-receivers in the German Bight.

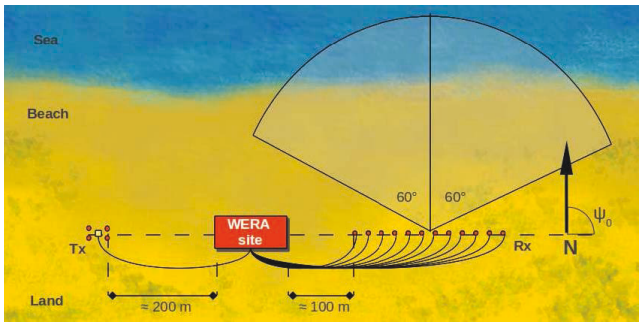

Figure 3.
Typical WERA system setup along a shore.

linear chirp with low phase noise, and is controlled by a high-speed counter. For completeness, a block diagram depicting the hardware realization of WERA is presented in Figure 4. Start and stop frequencies can be easily changed, thus allowing modifying both the mean carrier frequency and range resolution. The generated chirp is split into 13 or 17 channels, depending on the number of Rx antennas. One controls the transmitter and is amplified to 47 dBm, while the others are used for the phase-coherent I/Q demodulation. This is performed by 12 or 16 independent direct-conversion receivers. Before analog-to-digital (A/D) conversion, a low-pass filter suppresses those frequencies above Nyquist, while a high-pass filter attenuates the strong signals received directly from the Txs. The characteristics of the filters are measured and eventually compensated.

The successive steps of the data acquisition/display process are implemented in the software. The A/D converters are connected to a VME-bus and controlled by a CPU, which performs all the processing steps in real-time. The VME-bus system is connected to a digital Unix workstation by an Ethernet line, and measured raw data are directly stored on the workstation disks. The final processing, e.g. data storage, beamforming, direction finding, estimation of the sea surface current velocities, or vessel detection, is done directly on the workstation [16].

Figure 5 illustrates the built-in signal processing scheme implemented in WERA. After the A/D conversion of the complex demodulated signal, an interchannel amplitude calibration is applied to compensate the gain variations at the Rxs. Range resolution is obtained applying the fast Fourier transform (FFT) to all channels. The azimuth is resolved using a windowing function, usually the Hamming window, with linear Rx arrays, as described in [16]. In the case of a square Rx array, the direction finding algorithm is used instead [16]. An interchannel phase calibration is performed on the complex time series and the data are stored for further processing. Amplitude and phase calibrations are crucial for the accurate performance of azimuthal resolution techniques.

THE RANGE-DOPPLER POWER SPECTRUM

In the HF-band the contribution of sea clutter is produced by specific spectral components of the surface-height wave-field. Given a fixed azimuthal direction, the main features of the range-Doppler power spectrum (i.e., two visible lines extending along range) are due to first-order Bragg scattering and are generated by those gravity waves of half the radar wavelength, travelling towards and away from the radar site (Figure 6). These frequencies are valid in nonmoving waters and with respect to antenna look direction. In the presence of an underlying surface current, they can deviate from the theoretical values. Second-order Bragg scattering generates other side-band contributions, due to wave-spectrum. With increasing distance, sea clutter tends to become a white random process. In Figure 6, the power spectrum is evaluated from sample

field data, over a 512 samples recording interval (≈ 2 min).

The surface-wave propagation of the HF signal is influenced by several factors, including not only the transmitted power, but also the carrier frequency (i.e., with better propagation at lower frequencies), the sea-state, the water salinity and the temperature (jointly affecting the dielectric constant) and the possible presence of land. In addition to sea clutter, a variety of interference sources, both natural and man-made, can degrade the reception of ship echoes. Natural interference consists of unwanted propagation modes through the ionosphere (at lower HF frequencies and at ranges greater than 200 km), echoes from meteor trails and lightning. Radio frequency interference (RFI) is also present and manifests as vertical lines (i.e., almost constant along range and at given frequencies) in the range-Doppler spectrum. All these features can be observed in Figure 6; see also [20]. The main theoretical elements for modelling the backscatter signal can be found in [21], while the analysis and modeling of sea clutter and noise, both in the amplitude and frequency domains, can be found in [22], [23].

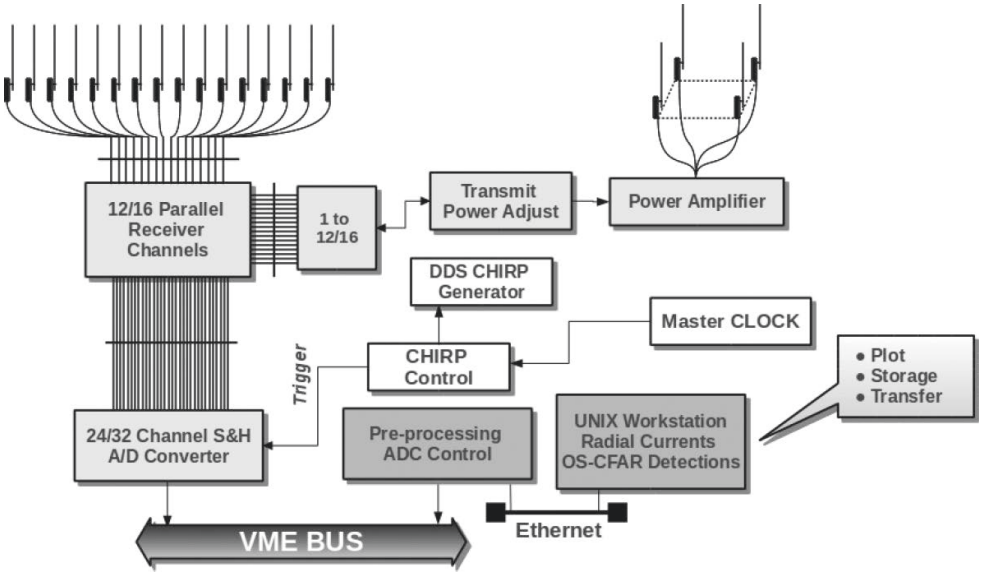

Figure 4.
WERA system description and main components.

THE HFSW RADAR EXPERIMENTS

The proposed MTT-DF network architecture is presented in two real study cases: the first in the Ligurian Sea, Mediterranean (see Figure 1(a)) [11], and a second in the German Bight, North Sea (see Figure 1(b)) [14]. The setup parameters of the radar systems are given in Table 1. The radars transmit and receive signals from the sea for about 56 min and then search for the best available RFI-free channel. This procedure is repeated every hour.

THE LIGURIAN SEA EXPERIMENT

STO CMRE conducted an experiment with two HFSW radars in 2009 to investigate the possibility of ship detection. Two WERA systems were deployed at the Italian coast of the Ligurian Sea, one on Palmaria Island near La Spezia (green) and another at San Rossore park near Pisa (red). The angles of the two antenna arrays were 296.2° and 12.0°, respectively. The radars and their coverage, which extends over an area of 150 km × 120°, are shown in Figure 1(a).

The two systems were operated using the same frequency at around f_0 = 12.5 MHz, but with orthogonal modulating waveforms for avoiding cross-interference. Range resolution was ΔR = 1.5 km, with a chirp bandwidth B = 100 kHz. It is important to note that the WERA on Palmaria Island was mounted at about 150 m above the mean sea level, on a rocky cliff going straight down to the sea. This was a quite unusual setup, since the HF

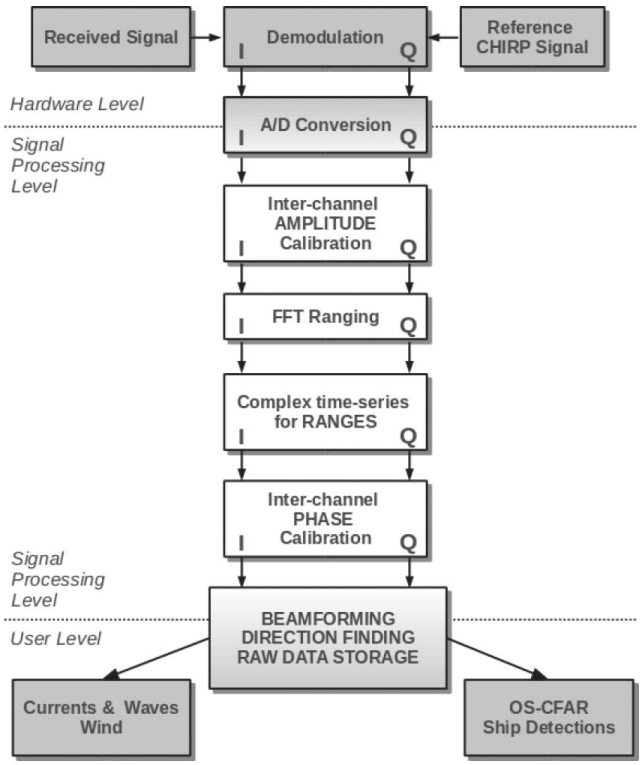

Figure 5.
WERA system processing scheme.

radars are mostly operated as close as possible to the sea. However, this specific installation granted better results in terms of coverage than the setup at San Rossore, as discussed in [11]. A possible explanation can be found in the significant contribution of the line-of-sight propagation and, probably, also in the more favourable ship-sensor geometries.

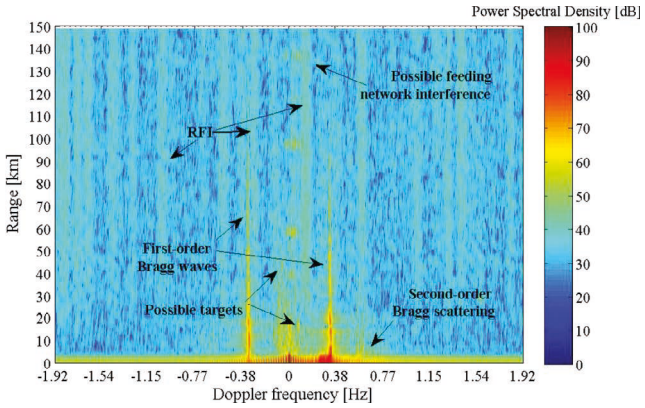

Figure 6.
Typical range-Doppler power spectrum in the HF-band.

THE GERMAN BIGHT EXPERIMENT

The second experimentation is currently ongoing in the German Bight. Here, three WERA radars are installed at Büsum (red) and on the islands of Wangerooge (magenta) and Sylt (green). The three HFSW radar sites and their areas of coverage are shown in Figure 1(b). Sylt and Büsum share the same frequency carrier f_0 and transmit with orthogonal modulating waveforms. In this specific case, the three HFSW radars are operating as part of the experimental Coastal Observing System for Northern and Arctic Seas (COSYNA) [24]. This operational integrated system combines observations and numerical models for the German Bight sea, for monitoring the status of both the sea and the shores. In this context, the HFSW radars are operated to measure currents and wave parameters and are successively assimilated to numerical modelling algorithms. This information is aimed to detect or predict possible variations and changes in the ecosystem, in the water quality and the effects that these can have on both the local and global climate. However, this region of the North Sea is also one of the busiest areas in the world in terms of maritime traffic. This is ideal for testing the proposed network architecture and for stressing it in a scenario dense with targets.

THE AIS DATA

Reasonably, the majority of boats and ships moving inside the so-called exclusive economic zones (EEZ) are cooperative. Depending on their size and type, some of these can be equipped with one, or more, transponder-based position-reporting systems. In the AIS message, a VHF transponder repeatedly broadcasts the ship name, position and other details for automatic display on nearby ships equipped with AIS. This allows ships to keep track of other ships in their immediate vicinity, while coastal authorities are also able to receive, plot and log the data from AIS base stations (BS) and repeaters. As established by the International Maritime Organization (IMO), AIS transponders transmit at 161.975 Mhz and 162.025 Mhz, and there are two classes of transmitters: A (min 12 W) and B (min 2 W). The transmission rate can vary between 2 s and 180 s for class-A, and 30 s for class-B. The coverage of a single transponder is expected to be in the order of tens of nautical miles, depending on the capability and coverage of the installed BS. However, while most targets will be cooperative, a smaller but still significant number is expected to be noncooperative, or too small to carry an AIS system.

STO CMRE collects historical AIS data directly from the Maritime Safety and Security Information System (MSSIS)

Table 1.

Setup Parameters of the HFSW Radars in the two Campaigns

Setup Param.	Palmaria	San Rossore	Wangerooge	Sylt	Büsum
Operation period	2009 – 2010	2009 – 2010	2010 – *ongoing*	2010 – *ongoing*	2010 – *ongoing*
Longitude E	9° 50′ 36″	10° 16′ 52″	7° 55′ 8″	8° 16′ 59″	8° 51′ 28″
Latitude N	44° 2′ 30″	43° 40′ 53″	53° 47′ 25″	54° 47′ 19″	54° 7′ 10″
h_0 *a.m.s.l.* [m]	150.0	0.0	0.0	0.0	0.0
ϕ_0 [°]	296.2	12.0	97.0	5.0	349.0
f_0 [MHz]	12.5	12.5	12.2 – 13.5	10.8	10.8
λ_0 [m]	24.0	24.0	24.6 – 22.2	27.8	27.8
T_c [s]	0.26	0.26	0.26	0.26	0.26
B [kHz]	100.0	100.0	100.0	100.0	100.0
ΔR [km]	1.50	1.50	1.50	1.50	1.50
sweep sign	up	down	up	down	up
Rx antennas	16	16	16	12	12

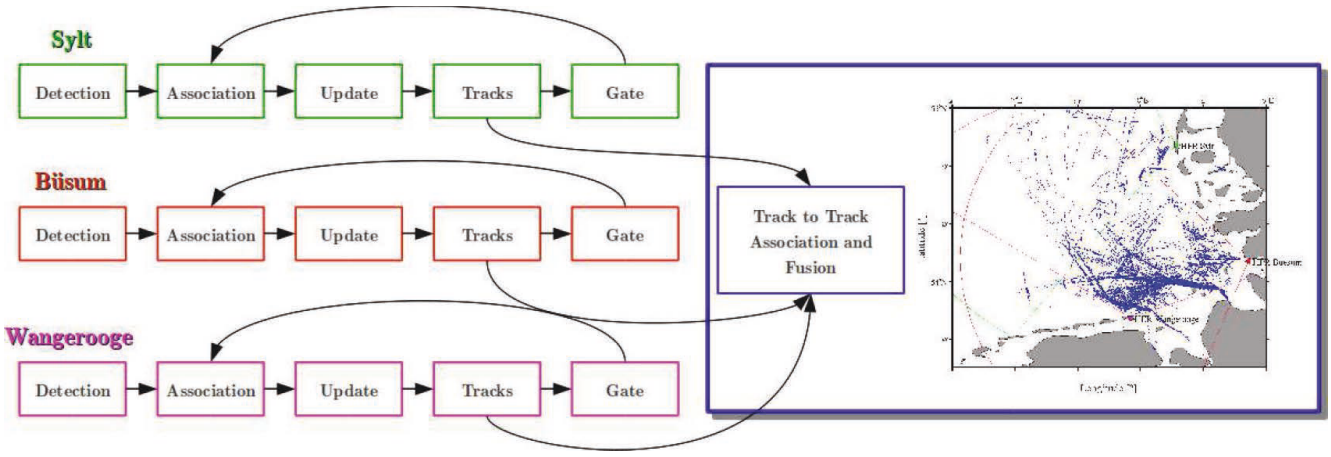

Figure 7.
Setup of the proposed MTT-DF processing chain with three sensors in the German bight.

sensor networks, from other external providers and from single ground-based stations. These navigation data, together with other experimental data, are used for scientific purposes, for developing algorithms and testing systems. Among the possible applications, a tool, named Traffic Route Extraction for Anomaly Detection (TREAD), has been recently developed [25]. The aim is to obtain, from the historical data, automated knowledge about the maritime traffic and main vessel routes. In this context, the possibility of combining AIS and HFSW radar data for vessel detection, tracking and classification is currently investigated. Having access also to navigation information could be precious for developing KB approaches to the MTT-DF problem [26], for discriminating noncooperative targets and/or possible threats, for providing useful information for anomaly detection or malicious behaviours [27], and for assessing system performance [11].

THE PROPOSED MTT-DF SYSTEM

THE PROCESSING CHAIN

The processing chain is depicted in Fig. 7, for the three-sensor German Bight scenario. In the first step, radar observations undergo a quality check and RFI removal. Target detection is then performed by the 3-D ordered statistic constant false alarm rate (OS-CFAR) algorithm presented in [9]. Coherent processing intervals, not statistically independent, are made of 512 samples with an overlap of 75%, i.e., a detection occurs every 33.28 s. These steps are directly performed by the WERA workstation at each site and then data are transmitted to CMRE databases in real-time. The MTT strategy is based on the joint probabilistic data association (JPDA) paradigm, i.e., a Bayesian approach which associates all the validated measurements to the tracks by probabilistic weights [3]. The track initiation/confirmation and track termination logics are respectively based on the 2/2&*M*/*N* and *N**/*N** criteria [3], while the filtering stage is performed by the unscented Kalman filter (UKF). The use of the UKF is motivated in [10] based on the discussion in [28] related to the polar to Cartesian coordinate transformations and the study reported in [29]. Indeed, the use of range-rate measurements (correlated to the range measurement [30]), as reported in [29], would recommend to work with the UKF (instead of extended Kalman filter (EKF) and converted measurement-Kalmann filter (CM-KF) especially because in the case the same order of computational effort would be required [31].

The confirmed tracks generated by the MTT at each site are then combined by means of a track-to-track (T2T) association and fusion logic [3]. Better results, in terms of time-on-target (ToT) and estimation accuracy, have been achieved compared with the single sensor outputs [11]. Further information about the algorithms and the system parameters can be found in [11] and [14] for the two study cases, respectively.

TARGET MOTION AND MEASUREMENT MODELS

The target state vector $\boldsymbol{x}_k$ at time k is defined in Cartesian coordinates $\boldsymbol{x}_k = \left[x_k, \dot{x}_k, y_k, \dot{y}_k\right]^T$ where x_k, y_k and $\dot{x}_k, \dot{y}_k$ are the position and velocity components along x,y directions, respectively. The nearly constant velocity (NCV) model is used to model the motion of large vessels [3]. The state-update equation is

$$\boldsymbol{x}_k = \boldsymbol{F}_k \boldsymbol{x}_{k-1} + \boldsymbol{\Gamma}_k \boldsymbol{v}_k. \tag{1}$$

The motion relation matrices $\boldsymbol{F}_k = diag([F_k, F_k])$ and $\boldsymbol{\Gamma}_k = diag([\Gamma_k, \Gamma_k])$ are described by (3), and where $(\times)^T$ and $diag(\times)$ are the transpose and diagonal matrix operators, respectively, while $T_k \triangleq T$ is the time interleaved between sampling times $k-1$ and k. Vector $\boldsymbol{v}_k$ accounts for unmodelled target accelerations and is assumed to be Gaussian with zero-mean and covariance matrix $\boldsymbol{Q}_k = diag\left(\sigma_v^2, \sigma_v^2\right)$. The measurement vector $\boldsymbol{z}_k$ is defined as $\boldsymbol{z}_k \triangleq \left[z_k^r, z_k^b, z_k^{\dot{r}}\right]^T$, where $z_k^r, z_k^b, z_k^{\dot{r}}$ are the measured range, bearing, and range rate. The target-originated measurement equation is thus

$$\boldsymbol{z}_k = \mathbf{h}\left(\boldsymbol{x}_k\right) + \boldsymbol{n}_k, \tag{2}$$

where

$$F_k = \begin{bmatrix} 1 & T_k \\ 0 & 1 \end{bmatrix}, \Gamma_k = \begin{bmatrix} T_k^2/2 \\ T_k \end{bmatrix},$$
$$\mathbf{h}(\boldsymbol{x}_k) \triangleq \begin{bmatrix} \sqrt{x_k^2 + y_k^2}, \arctan\left(\frac{y_k}{x_k}\right), \frac{x_k \dot{x}_k + y_k \dot{y}_k}{\sqrt{x_k^2 + y_k^2}} \end{bmatrix}^T \quad (3)$$

with $\mathbf{h}(.)$ being the measurement function. The instrument noise vector $\boldsymbol{n}_k$ is assumed to be Gaussian with zero-mean and diagonal covariance elements σ_r^2, σ_b^2, and $\sigma_{\dot{r}}^2$. In literature its elements, i.e. $n_k^r, n_k^b, n_k^{\dot{r}}$, are all assumed to be statistically independent, except for n_k^r and $n_k^{\dot{r}}$, which have correlation coefficient ρ. This correlation index can be computed and the range-Doppler offset compensated, as described in [32].

THE MTT PROCEDURE

Let us assume that at time k a set of tracks are active/preliminary $\mathcal{T}_k = \{T_1(k), \ldots, T_J(k)\}$, where $T_j(k)$ is a natural number defining the identifier (ID) of the j^{th} track. A validation gate region $\mathcal{G}_j(k)$, for all $j = 1, \ldots, J$, is constructed. Given that the target-originated measurements are Gaussian distributed around the predicted measurement $\boldsymbol{z}_{k|k-1}^j$ of target j, the gate is [3]

$$\mathcal{G}_j(k) = \left\{ z : \left(z - \boldsymbol{z}_{k|k-1}^j\right)^T \left(\boldsymbol{S}_k^j\right)^{-1} \left(z - \boldsymbol{z}_{k|k-1}^j\right) < \gamma \right\}, \quad (4)$$

where $\boldsymbol{S}_k^j$ is the innovation covariance of the predicted measurement, while the threshold γ determines the gating probability P_G, i.e., the probability that a measurement originated by target j is correctly validated.

Track Management

With no loss of generality, track management can be roughly divided into three main steps: track initiation, track update and track termination. In the track initiation phase, a measurement is associated to the track $T_j(k)$ if it satisfies (4). Every unassociated measurement is called initiator and yields a tentative track, which becomes preliminary if a detection falls in the gate at the next timestamp (2/2 logic), otherwise the track is dropped. For each preliminary track, the JPDA-UKF can be initialized and used to set up a gate for the next sampling time, see (4). Starting from the third scan, a logic of M detections out of N scans is used for the successive validation gates. If at scan $N + 2$ the logic requirement is satisfied, the track becomes active, otherwise it is terminated.

In the track update phase, for each active and preliminary track, the target state is updated applying the JPDA-UKF, as described in [11]. In the track termination phase, an active track is terminated if no detections have been validated in the past N^* most recent sampling times, if the track uncertainty has grown too much, or if the target has reached an unlikely maximum velocity v_{max}.

Target State Prediction and Update

Given the target state and its covariance at time $k - 1$, the predicted state and its covariance are obtained using the algorithms summarized in [11]. In the data association phase, a validation matrix is set up for all the targets, both preliminary and active. Rows and columns of each matrix are indicized with all the validated measurements falling in the gate, also considering the case of no-measurements. From the validation matrix, all the feasible joint association events are constructed, assuming that each measurement is generated from a target or from clutter, and that each target generates at most one measurement, with detection probability P_D. The probabilities of the joint events are evaluated assuming that the target-originated measurements are Gaussian distributed around the predicted location of the corresponding target measurement, and that the false alarms are distributed in the surveillance region according to a Poisson point process of parameter Λ, The association probabilities of target j with measurement i, namely β_{ij}, are obtained from the joint association probabilities. Details can be found in [3], [33]. In the update phase, the target state at time k and its covariance are updated by averaging the UKF updates with the association probabilities β_{ij}. All the parameters of the MTT system are given in Table 2.

Table 2.

MTT Parameters		
Parameter	**Value**	**Specification**
T_k	16.64s/33.28s	Sampling period
σ_v	1×10^{-2} ms^{-2}	Std of process noise
σ_r	150 m	Std of range meas.
σ_b	1.5°	Std of bearing meas.
$\sigma_{\dot{r}}$	0.1 ms^{-1}	Std of range-rate meas.
P_D	0.35	Detection probability
Λ	10^{-9} m^{-2}/scan	Clutter density
γ	3.3^2	Gate threshold
$\sigma_{x,y}$	500 m	Init. filter (pos.)
$\sigma_{\dot{x},\dot{y}}$	10 ms^{-1}	Init. filter (vel.)
v_{max}	25 ms^{-1}	Maximum velocity
M/N	7/8	Track confirmation logic
N^*/N^*	3/3	Track termination logic

DATA FUSION PROCEDURE

The T2T paradigm, which is the core of the DF strategy, can be divided into T2T association and T2T fusion [3] procedures.

T2T Procedure

The multidimensional assignment (MDA) approach can be applied both to single- and multiple-sensor data association problems [4]. The problems of single-sensor data association over multiple scans and single-scan over multiple sensors can be

equivalently addressed resorting to the Lagrangian relaxation method [34]. At each new time scan k, each sensor produces its own set of $M_n(k)$ observations (i.e. the track contacts), where n = 1, 2, 3. For brevity, we will omit k. With the binary variable $z_{i_1 i_2 i_3}$ we define the track formation hypothesis for which observations i_1, i_2, and i_3 are originated from the same target. This variable is 1 if the track association is correct, 0 otherwise. A dummy association (the index is set to zero) corresponds to a missed detection event. Thus, the final data association problem will be made by such track-to-track hypotheses, which account for all the sensor observations. Similarly, we define $c_{i_1 i_2 i_3}$ as the track formation cost [11].

The optimization problem presented in [4] becomes, in the case of three sensors, the minimization of an objective function $v(\delta)$ defined by

$$v(\delta) = \mathbf{min}_{\delta_{ijl}} \sum_{i=0}^{M_1} \sum_{j=0}^{M_2} \sum_{l=0}^{M_3} c_{ijl} \delta_{ijl}, \tag{5}$$

subject to the constraints

$$\sum_{i=0}^{M_1} \sum_{j=0}^{M_2} \delta_{ijl} = 1, \qquad \forall l = 1, \ldots, M_3, \tag{6a}$$

$$\sum_{i=0}^{M_1} \sum_{l=0}^{M_3} \delta_{ijl} = 1, \qquad \forall j = 1, \ldots, M_2, \tag{6b}$$

$$\sum_{j=0}^{M_2} \sum_{l=0}^{M_3} \delta_{ijl} = 1, \qquad \forall i = 1, \ldots, M_1. \tag{6c}$$

Let us define with u_l the l^{th} Lagrange multiplier, where l = 0, …, M_3 and $u_0 = 0$. In the Lagrangian relaxation approach, we can remove one set of constraints, e.g. (6a), using the Lagrangian multipliers in the original objective function [see (5)]. This reduces the 3-D to a 2-D assignment problem. The proper choice of the Lagrangian multipliers tends instead to force the satisfaction of the constraints. The iterative procedure is described in [14] and further details in [4].

Note that possible measurement bias, see e.g. [32], has been compensated in the filtering and considered negligible here during the T2T association procedure. However, in the long run all the sensors can exhibit registration errors, and in this case the MDA approach should be enhanced with more advanced techniques able to compensate such registration errors between the radar systems, see e.g. [35].

THE KB TRACKING METHODOLOGY

Recently, it has been shown that the tracking stage can effectively take advantage of a priori information on ship traffic [26]. This concept is known as KB tracking. Considering the historical AIS contacts, we can observe that there are some geographical regions where most of the maritime traffic is concentrated. These regions are the so-called sea lanes or routes. In [26] a variable structure interactive multiple model (VS-IMM) tracking procedure has been proposed to mitigate track fragmentation, mostly caused by the target obscuration phenomenon. In the case of ground target tracking, target obscuration can be provoked by the presence of hills or tunnels, which hide the target from the sensors point of view. In our case, this effect is present when the radar is turned off to reallocate operative HFSW frequencies, when there is a low signal-to-clutter ratio (e.g. when the target is moving in the Bragg scattering region), and when the target aspect angle produces a weak return.

The specification of a ship sea lane map can be tabulated including sea lane segments, visibility conditions, and initial/final points of sea lanes. Unlike an off-sea lane target, which is free to move in any direction, the motion of an on-sea lane target is highly constrained. To handle motion along the sea lane, the concept of directionally dependent noise is introduced [36]. For on-sea lane targets, the constraint means more uncertainty along the route than orthogonal to it.

Extensive simulations were performed in [36]. Different algorithms were analyzed in the context of ground tracking. However, the best performance was obtained using VS-IMM, able to handle the on/off-road transitions and the change from one road to another more smoothly than the fixed IMM. In addition, once the target begins to move along a road, the VS-IMM yields better course estimate than the fixed IMM, which uses only an open field model [37]. In [26], a significant improvement of the KB-tracking procedure, in terms of system performance, has been demonstrated in comparison with the standard approach recently presented in [11]. On the other hand, a gain in terms of ToT can be observed without losing in terms of false alarm rate (FAR).

THE MSA VIEWER

STO CMRE is developing a tool, named MSA viewer [38]–[40], which is a Web browser map application integrating different data and fusion services, and relying on a service-oriented architecture (SOA) implementation. This work, which takes forward the NATO Network-Enabled Capability (NNEC) concept, is designed to allow information to be available and useful to all authorized users, with the main objectives of supporting operations in a network-enabled environment and providing users with a better comprehension of the maritime picture. The services granted by this tool can be classified in data (e.g. data from different sensors and sources), and fusion services, (e.g. providing with the capability of fusing radar data). The idea is to increase the degree of automation, in order to provide the operator with useful information and to help her during the decision-making process.

The tool exploits an SOA architecture for sharing, processing and visualizing big data in the MSA domain. This architectural model permits the development of distributed applications. These make use of the Windows Communication Foundation (WCF) [41] which is a Microsoft framework for building reliable, secure and interoperable distributed applications. The WCF implements many advanced Web service standards, and enables interoperability with other Web services built on different platforms.

The MSA viewer provides users with a graphical visualization of the maritime scene, by integrating it with geospatial information. Users can visualize both real-time and historical vessel

traffic from different data sources, and combine data by using data fusion algorithms and other integration services. The user interacts with the viewer through an interface to control the input, the processing and the visualization of maritime data. However, it is important to say that the viewer is not a command and control system, and has no operational capabilities. As mentioned, it has been developed solely for scientific purposes. However, using a standard workstation, we are able to achieve quite good real-time performance; basically we can always process the radar data faster than real-time (depending on the amount of ship traffic) and visualize the output by the MSA viewer. The main computer language is *C#*. Furthermore, the algorithm kernel is implemented in Matlab. Algorithmic routines interact with *C#* framework by using an ad hoc interoperability module developed at CMRE.

Two sample snapshots describe the maritime pictures in the Ligurian Sea and German Bight, as shown in Figures 8 and 9, respectively. The fused HFSW radar tracks (blue) and their uncertainty ellipsoids can be superimposed to the AIS routes (red). As we can observe, the amount of traffic is far greater in the second case and many radar tracks have no corresponding AIS report. Therefore, in such a context it is important to discriminate false tracks and to provide a measure of noncooperative ship traffic. However, this suggests that HFSW radars can provide a supplementary coverage for regions not covered by the AIS navigation-reporting system.

EXPERIMENTAL RESULTS

ANALYSIS OF THE RADAR TRACKS

The two scenarios are analyzed in Figures 8, and 9, respectively, for the Ligurian Sea and German Bight campaigns. In the first study case (see Figure 8), AIS data and fused tracks from the two radars were recorded on May 8, 2009, during the interval 13:00 – 14:00 UTC. As we can observe, there is a good coverage of the AIS system, thanks to a BS receiver mounted at Castellana, at about 180 m above the mean sea level. Figure 9 shows instead the AIS available dataset and the T2T system exploiting contemporaneously the three HFSW radar systems in the second study case, with data recorded on Aug. 1, 2013, during the interval 12:00 – 13:00 UTC. In this case, the coverage of the AIS data is limited to the coastal areas, with the exception of a few trajectories. However, in both cases, most of the main traffic routes are well tracked by the MTT-DF system. In fact, there is a good agreement between the estimated tracks and the available ground-truth trajectories represented by the AIS system. In addition, a lot of maneuvering ships can be observed closely moving in front of Wangerooge, entering and leaving the main traffic lanes. Thus, each particular MS application scenario could require a different MTT-DF solution to address the vessel detection and tracking problems.

VALIDATION OF THE RADAR TRACKS

Omitting the time index, the AIS report $\mathcal{X}^{AIS}$ represents the set of the target state vectors $\boldsymbol{x}^n$ during a given recording interval $\mathcal{X}^{AIS} \triangleq \{\boldsymbol{x}^n\}_{n\in\mathcal{N}}$, where $\mathcal{N}$ is the list of ships reporting their static and kinematic information in the same interval. Kinematic information, i.e., longitude, latitude, course-over-ground (COG) and speed-over-ground (SOG), are converted into the Cartesian data vector. Each AIS data vector is filtered and interpolated at the radar timestamps, thanks to the high data-rate of the AIS w.r.t. the radar. However, it is possible that no AIS information from the vessel is received for a long period of time. In this case the interpolated route could not represent a meaningful ground-truth anymore. For this reason, in order to eliminate these cases we define a flag index I_m^n, which is 1 if $\Delta T_m^n \le \Delta T_{max}$, and 0 otherwise. Here m represents the time instant τ_m^n at which the n^{th} ship transmits its position, and $\Delta T_m^n = \tau_m^n - \tau_{m-1}^n$ is the time interval between two AIS transmissions of the n^{th} vessel. The parameter ΔT_{max} represents the maximum acceptable time from the last report. In the time interval when $I_m^n = 0$ the AIS data from the n^{th} vessel are not used for performance evaluation. With no loss of generality, detections (e.g. OS-CFAR) and tracks (e.g. JPDA-UKF and T2T), can be considered as the target state estimates at time k, i.e,. $\mathcal{X}_k^{HFSW} \triangleq \{\boldsymbol{x}_k^j\}_{j\in\mathcal{T}_k}$, where $\mathcal{T}_k$ is the set of detections for the OS-CFAR or the set of confirmed tracks for the JPDA-UKF and T2T at time step k.

An association procedure between the AIS and the radar data is required to compute the system performance. At time k each AIS contact $\bar{\boldsymbol{x}}_k^n \in \mathcal{X}_k^{AIS}$, with $n \in \mathcal{N}_k$, is associated to a single track contact $\hat{\boldsymbol{x}}_k^j \in \mathcal{X}_k^{HFSW}$, with $j \in \mathcal{T}_k$. The association is carried out by searching the nearest among all the HFSW radar reports falling inside a 3-D (range, azimuth, range-rate) performance validation region (PVR) centered on the AIS contact

$$\left(\mathcal{T}_k \ni j \to n \in \mathcal{N}_k\right) : d\left(\hat{\boldsymbol{x}}_k^j, \bar{\boldsymbol{x}}_k^n\right) = \min_{i\in\mathcal{T}_k} d\left(\hat{\boldsymbol{x}}_k^i, \bar{\boldsymbol{x}}_k^n\right) \tag{7}$$

The j^{th} radar contact is validated if this distance, represented by the operator $d(.,.)$, is below a given threshold. If the n^{th} AIS report has a validated track contact, we have a correct detection, otherwise a missed detection. At a given k, the single AIS report can be associated with at most one radar report. All the radar contacts, which are not validated in this way, are instead false alarms.

STATISTICAL ANALYSIS

The detection and tracking capabilities of the proposed MTT-DF system can be evaluated quantitatively by using the metrics proposed in [11]. These performance metrics have been defined to compare the signal processing chain from the detection to the fusion stages. Among these, we have 1) the pair ToT and FAR, 2) the track fragmentation, and 3) the root mean square error (RMSE) of the target position and velocity. The ToT is the percent of time that a target is successfully observed by the system, while the FAR is the normalized number of false track contacts (or detections) generated in the surveillance region per unit of space and time. The track fragmentation is quantitatively characterized by the ToT and the number of subtracks associated with the same target. Ideally we would like to have 100% as ToT with just one single track, while in a real scenario this is very rare. At last, the RMSE measures the accuracy of the radar system. Tracks

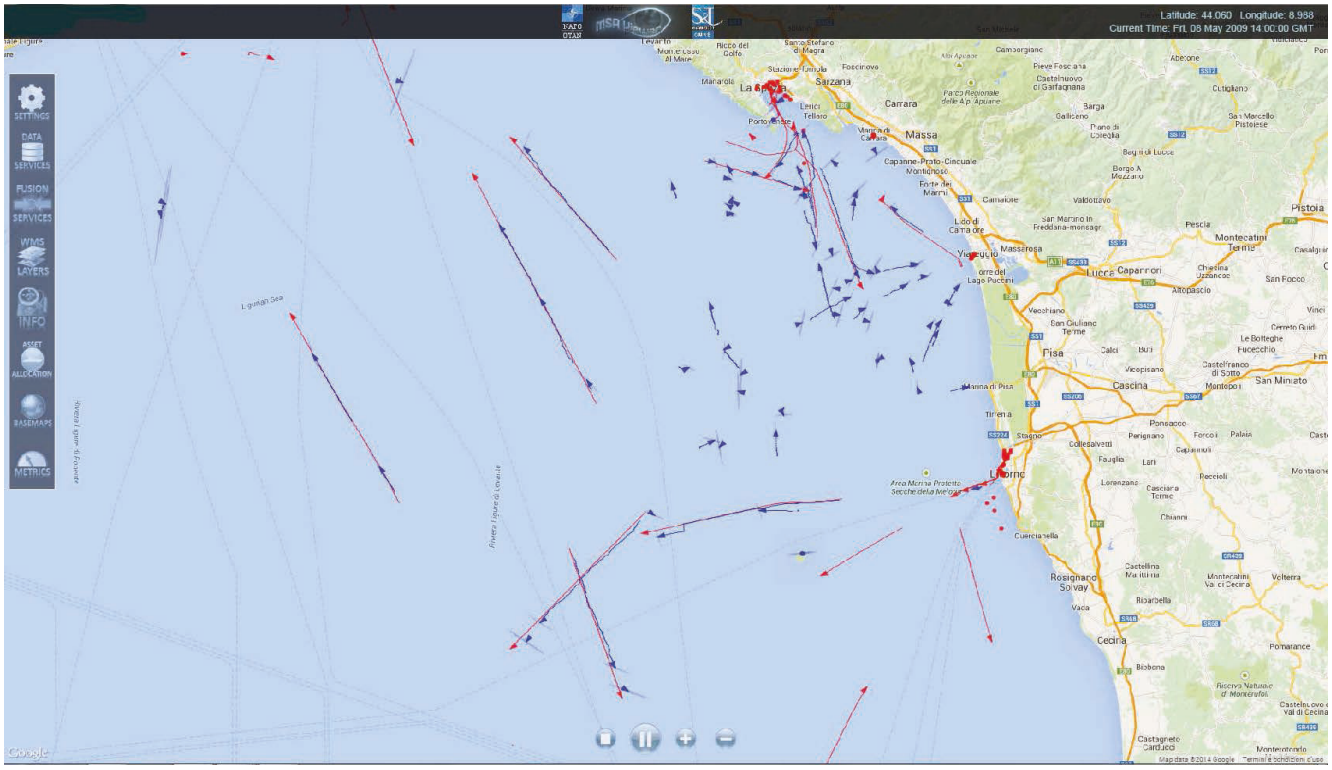

Figure 8.
The Ligurian Sea MSA picture using the viewer: AIS contacts (red), T2T system tracks (blue).

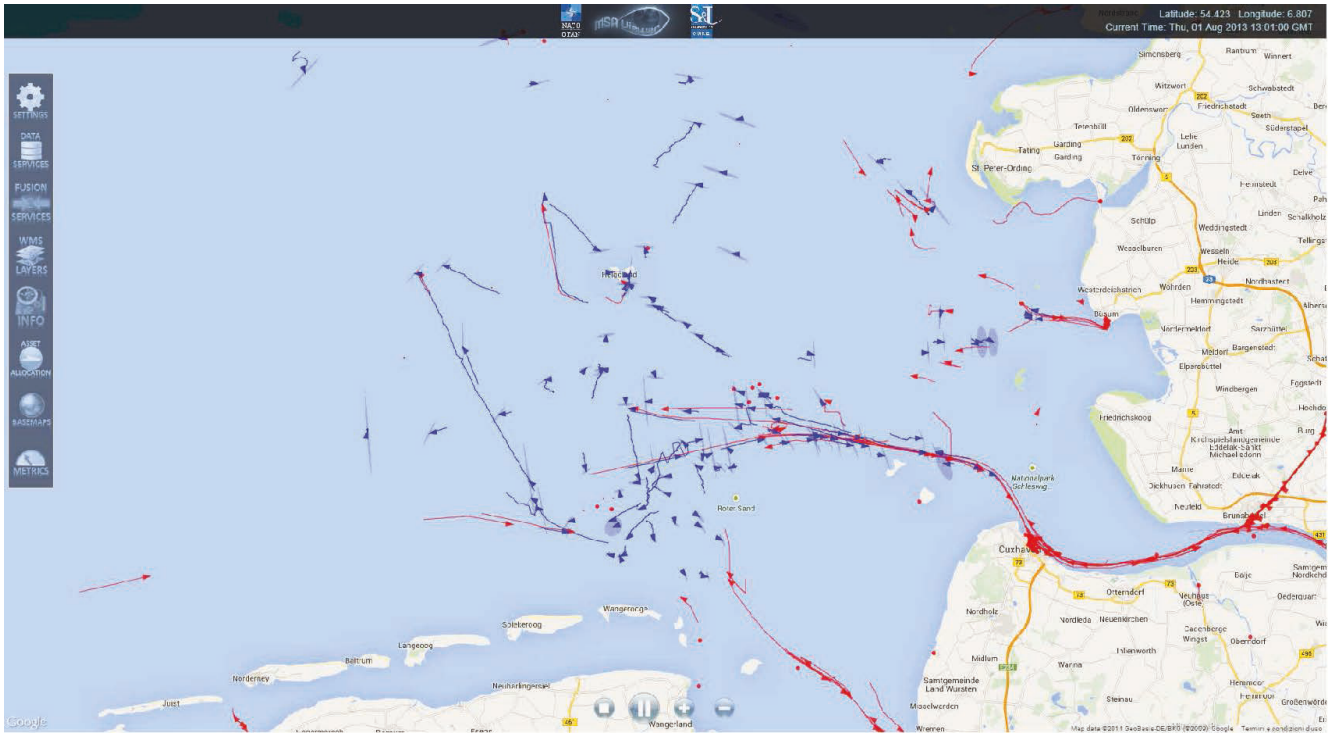

Figure 9.
The German Bight MSA picture using the viewer: AIS contacts (red), T2T system tracks (blue).

and detections are validated or labeled as false using the AIS ship reports from the AIS. Unfortunately there are also several vessels from which, for a number of reasons, we do not receive any AIS reports. Thus, the FAR we consider represents the worst case.

In Figure 10, the ToT confidence intervals, depicting the mean and standard deviation, are estimated and represented for ship lengths of multiples of 50 m. Results from the Ligurian Sea experiment are averaged over the defined range, azimuth and range-rate intervals and over a recording interval of 29 days. As expected, an increase in the ship length brings an increase in the ToT. This is especially clear for very large ships, i.e. those longer than 250 m. The data fusion strategy improves the ToT of about 5–10% for Palmaria and 15–25% for San Rossore on average. This result suggests that the T2T procedure relies more on the Palmaria tracker than on the San Rossore one. Moreover, it gives us confidence that the main issues related to single-operating HFSW radars can be overcome by multiple sensors, with no additional costs [7], [11].

In Figure 11, the same ToT confidence intervals are evaluated for the German Bight experiment, over a recording interval of 38 days. The radar at Sylt was under maintenance for the most of the period and could not offer a satisfying statistical dataset. The same increasing trend shown in Figure 10 can be observed, however with some clear differences. The capability of the systems is significantly smaller than in the previous experiment. This fact can be explained by the different traffic scenarios, in which several ships move in cluster-like trajectories. The MTT-DF system is limited by the inherent low resolution of the radars. The environmental issues that affect this region could be a further reason for the degradation of the performance. The two standalone sensors have similar performance, and the final T2T output seems not to rely mostly on one of the two.

As known, the ToT is related to the FAR, as an increase in the probability of detection bears an increase in the probability of false alarm. In the scatterplot analysis of Figure 12, which refers to the experiment in the Ligurian Sea, the green circles and squares represent instead the two JPDA-UKF outputs, while the blue triangles are the output pairs of the T2T system. In terms of ToT, the JPDA-UKF (green circles and squares) provides results comparable to those of the detection algorithm (red circles and squares). However, most of the false alarms are pruned and the FAR is about one order of magnitude smaller. Finally, the T2T cloud (blue triangles) spreads along larger ToTs, with intermediate FARs, even if its distribution is closer to the JPDA-UKF of Palmaria than of San Rossore. In conclusion, the OR fusion strategy allows to improve single-sensor performance, but the increased system detection capabilities are paid in terms of increased number of false tracks [11].

BENEFITS FROM THE APPLICATION OF KB TRACKING

In this section the use of a KB tracking methodology that takes advantage of a priori information on the ship traffic is presented, see [26], [42], [43]. This a priori information is given by the ship sea lanes and by their related motion models, which together constitute the basic building blocks of a VS-IMM procedure. False

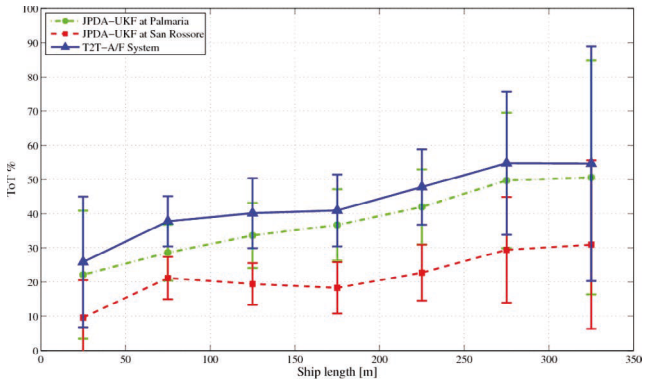

Figure 10.
Confidence intervals for the ToT vs ship length from the Ligurian Sea dataset: JPDA-UKF at Palmaria (green) and San Rossore (red), T2T system (blue).

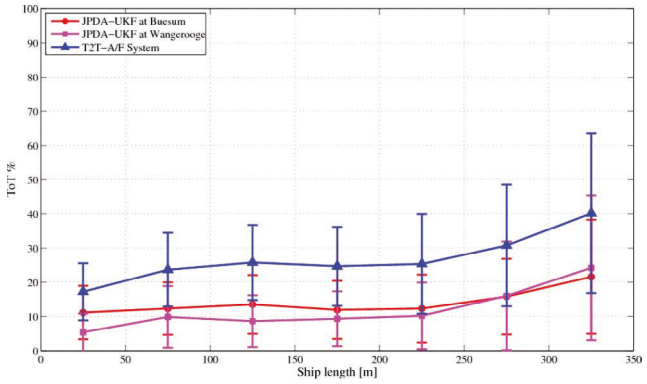

Figure 11.
Confidence intervals for the ToT vs ship length from the German Bight dataset: JPDA-UKF at Büsum (red) and Wangerooge (magenta), T2T system (blue).

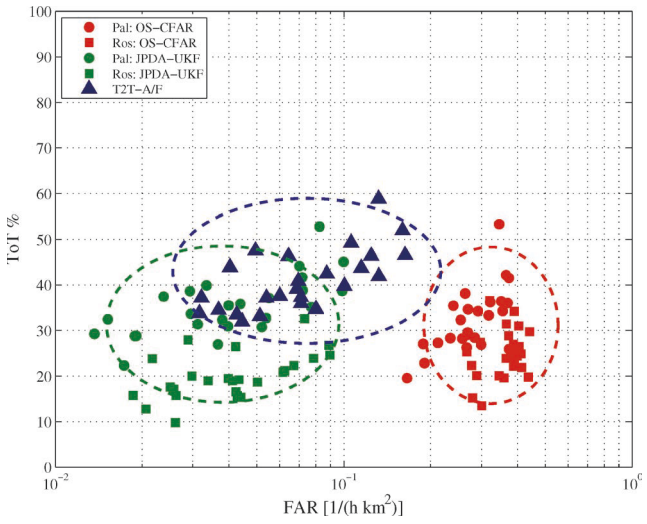

Figure 12.
ToT vs FAR scatterplot analysis: red circles (OS-CFAR at Palmaria), red squares (OS-CFAR at San Rossore), green circles (JPDA-UKF at Palmaria), green squares (JPDA-UKF at San Rossore), blue triangles (T2T). Values for each day are represented by empty symbols, averaged values are represented by full symbols. The dataset is from the Ligurian Sea experiment.

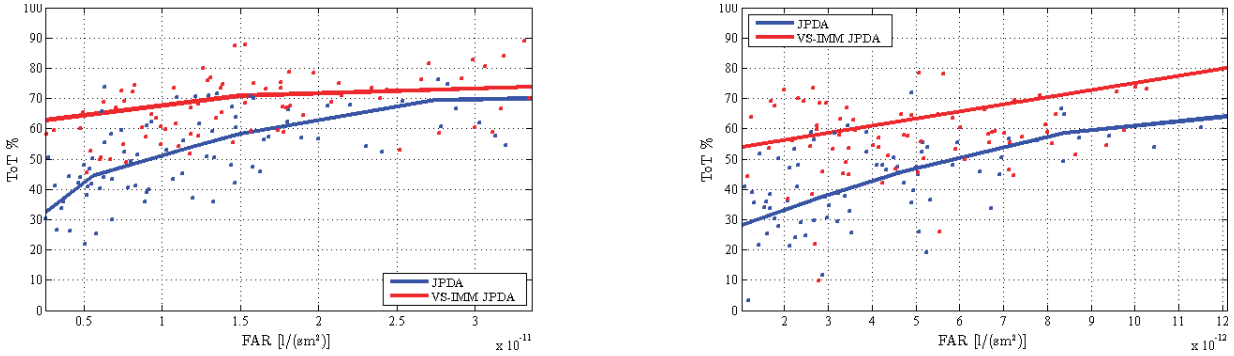

Figure 13.
ToT versus FAR at the varying of N*. Blues and red squares depict the daily values for the JPDA and the VS-IMM JPDA, respectively. Blue and red lines describe the convex-hull resulting curves obtained from these values. Subfigure (a): Palmaria; subfigure (b): San Rossore.

alarms and missed detections are dealt with using the JPDA rule and nonlinearities are handled by means of the UKF. The overall performance is defined in terms of ToT, FAR, track fragmentation, and accuracy. A full statistical characterization is provided using one month of data. A significant improvement of the KB-tracking procedure, in terms of system performance, is demonstrated in comparison with a standard JPDA tracker. The main improvement is the better capability of following targets without increasing the FAR. This increment is much more evident in the region of low FAR, where it can be over the 30% for both the HFSW radar systems. The KB-tracking exhibits on average a reduction of the track fragmentation of about the 20% and the 13% of the utilized HFSW-radar systems.

The analysis compares the behaviour of the VS-IMM JPDA-UKF and JPDA-UKF algorithms, at the varying of N^*, i.e., the variable characterizing the track termination logic. When the parameter N^* grows, the FAR and the ToT both increase, because the track termination requirement becomes less strict [26]. The choice of N^* has been done such that the daily FAR values of the two tracking algorithms are similar. Then, two cases have been considered: $N^* = 1$ and $N^* = 5$ for the VS-IMM JPDA-UKF algorithm and $N^* = 5$ and $N^* = 10$ for the standard JPDA-UKF, respectively. The daily ToT-FAR pairs are depicted by the full square markers, color-coded with blue for the JPDA-UKF and red for the VS-IMM JPDA-UKF, respectively. In both scenarios, the VS-IMM outperforms the standard JPDA in terms of both ToT and FAR. This result means that for each value of the FAR, the ToT of the VS-IMM is larger than the one of the JPDA. Moreover, it is worth observing that the ToT statistics are better than those described by the receiver operating characteristic (ROC) scatterplots in Figure 12. In fact, for this analysis only a number of radar tracks has been considered, i.e., those in the immediate vicinity of the selected AIS vessel routes. An average improvement of 10% can be achieved, as described in [26].

The gain we obtain by exploiting the information derived from the AIS routes is well represented by the solid line curves of Figure 13. The curves depict the convex hulls of daily pairs ToT-FAR, for the two radars at Palmaria [see Figure 13(a)] and San Rossore [see Figure 13(b)]. However, it is worth considering that those regions, which have the smallest values of FAR, represent the most important areas from an operative point of view. In these specific cases, the performance gap between the two approaches is larger, see Figure 13(a). Figure13 demonstrates how the performance gain advantages are more significant in the low false alarm region. However, the ToT improvement is larger in the case of San Rossore than in the case Palmaria. The reason must be found in the worse detection capability of the radar at San Rossore, as already pointed out in the previous sections and more extensively in [11].

CONCLUSIONS

In this work, an MS system based on multiple simultaneously operating low-power HFSW radars has been presented. The proposed radar systems could operate in more complex integrated maritime surveillance (IMS) systems, but also in combination with other kinds of data. In addition, they can effectively grant continuous-time wide-area coverage in a cost-effective manner. In the paper, two study cases have been analyzed and described. In the former case, two sensors have been deployed along the Ligurian coast of the Mediterranean Sea, while, in the latter, three radars are currently operated by HZG in the German Bight for measuring sea state parameters and surface currents. In both cases, the experimental data recorded by the radars have been demonstrated to provide reliable information on ship detection and tracking, with thus no additional costs on the system installation. A whole processing chain, consisting of a 3-D OS-CFAR detection algorithm, the JPDA-UKF tracking strategy and a T2T logic, has been considered to tackle the MTT-DF problem. A methodology for validating the output tracks, exploiting the AIS reports as ground-truth information, has been proposed and performance metrics have been evaluated for assessing the system performance. In the second study case, the data stream from the three stations is acquired in real-time and a web-based MSA viewer displays, from the operator's point of view, the maritime situation in the region of interest. Further results have been shown demonstrating the effectiveness of KB tracking exploiting historical ship trajectories, for overcoming the problem of vessel obscuration and increasing the final ToT with no additional costs in terms of FAR.

For these reasons, we think that the HFSW radar technology applied to the field of MS could be a cost-effective solution for granting continuous coverage of wide open-sea areas. Multiple sensors can exploit different ship-sensor geometries and, thus,

overcome most of the limitations deriving from the use of standalone sensors. In addition, they can grant coverage of large areas and provide tracks also for nonreporting ships or detect anomalies in the vessel routes. Information about vessel routes can be used to improve the final performance, thus providing a more choral vision of the MS scenario.

PERSPECTIVES

Despite the promising results, this analysis opens new research directions, all aimed to improve the system capability and confidence in the maritime picture. For instance, the reliability and coverage of the AIS reports could be monitored from radar data, as addressed in [27]. More advanced techniques could be used for tracking (e.g. based on multiple kinematic modes) and data association algorithms (e.g. exploiting the signal-to-clutter-ratio (SCR) information). Different types of sensors, as well as the AIS system itself, could be used to produce a more complete maritime picture of the region under analysis. This situation could require a different tracking algorithm, able to deal also with ship maneuvers, e.g. the interacting multiple model (IMM), see also [3]. As already observed, another problem is represented by the high density of the vessel traffic out of river Elbe and from the mainland and along the main traffic routes. Ship discrimination could be a possible problem for the low-resolution radar system, as well as the JPDA data association rule, which combines probabilistically all the neighboring contacts. Target tracking techniques, working with unresolved targets, which can be able to mitigate such kinds of problems are reported in [44], [45]. A different approach to the MTT problem could be to apply group-tracking or clustering algorithms, see e.g. [46], [47]. However, results should be presented and discussed also taking into account a number of different issues related to the maritime scenario, such as different meteorological and oceanographic (METOC) conditions affecting the signal propagation, different coastline profiles and high vessel traffic. Although their impact on the system performance has been qualitatively investigated [48], and a dependency has been shown between the system detection and tracking capabilities and the significant wave height, all these analysis directions are currently undergoing further investigations. Results of an adaptive tracker to environmental time-varying change have been reported in [49], [50]. Clearly, the solution in [49] exhibits a sensible improvement in terms of performance w.r.t. the nonadaptive strategy but at the cost of a sensible higher computational effort.

Some target tracking procedures could require an unreachable computational effort when a large number of detections per scan are provided if the targets are close to each other (there is an exponential complexity in the number of targets with overlapped gates). Scalable MTT solutions are under investigation in which the processing cost of several HF radars is linear in terms of both number of detections (targets/clutter) and number of radars, see e.g. [51]. ◈

ACKNOWLEDGEMENTS

This work was supported by the NATO Allied Command Transformation (NATO-ACT) under the Maritime Situational Awareness (MSA) project. Both the HFSW radar, part of the AIS and the meteorological and oceanographic (METOC) data were kindly made available through the COSYNA system, which is operated by Helmholtz-Zentrum Geesthacht in Germany. Moreover, our sincere gratitude goes to our STO CMRE colleagues Mr. Gianfranco Arcieri, Giampaolo Cimino, Leonardo Millefiori and Renato Sirola, for their help with the MSA viewer implementation and data transfer, and to Mr. Jonathan Locke and Steven Horn for their useful comments on the manuscript. Finally, we would like to acknowledge Dr. Gemine Vivone for his help with the KB tracking results.

REFERENCES

[1] Farina, A., and Studer, F. A. *Radar Data Processing. Vol. II - Advanced Topics and Applications.* NewYork: Wiley, 1986.

[2] Bar-Shalom, Y., and Rong Li, X. *Multitarget-Multisensor Tracking: Principles and Techniques.* Storrs, CT: YBS Publishing, 1995.

[3] Bar-Shalom, Y., Willett, P., and Tian, X. *Tracking and Data Fusion: A Handbook of Algorithms.* Storrs, CT: YBS Publishing, 2011.

[4] Blackman, S., and Popoli, R. *Design and Analysis of Modern Tracking Systems.* Norwood, MA: Artech House, 1999.

[5] Mahler, R. *Statistical Multisource-Multitarget Information Fusion.* Norwood, MA: Artech House, 2007.

[6] Braca, P., Marano, S., Matta, V., and Willett, P. Asymptotic efficiency of the PHD in multitarget/multisensor estimation. *IEEE Journal of Selected Topics in Signal Processing,* Vol. 7, 3 (2013), 553–564.

[7] Braca, P., Vespe, M., Maresca, S., and Horstmann, J. A novel approach to high frequency radar ship tracking exploiting aspect diversity. In *Proceedings of the IEEE International Geoscience and Remote Sensing Symposium* (IGARSS), Munich, Germany, 2012.

[8] Gurgel, K.-W., Antonischki, G., Essen, H.-H., and Schlick, T. Wellen radar (WERA), a new ground-wave based HF radar for ocean remote sensing. *Coastal Engineering,* Vol. 37, 3 (Aug. 1999), 219–234.

[9] Dzvonkovskaya, A., Gurgel, K.-W., Rohling, H., and Schlick, T. Low power high frequency surface wave radar application for ship detection and tracking. In *Proceedings of the IEEE International Radar Conference,* Adelaide, Australia, Sept. 2008.

[10] Braca, P., Grasso, R., Vespe, M., Maresca, S., and Horstmann, J. Application of the JPDA-UKF to HFSW radars for maritime situational awareness. In *Proceedings of the* 15th *International Conference on Information Fusion* (FUSION), Singapore, 2012.

[11] Maresca, S., Braca, P., Horstmann, J., and Grasso, R. Maritime surveillance using multiple high-frequency surface-wave radars. *IEEE Transactions on Geoscience and Remote Sensing,* Vol. 52, 8 (Aug. 2014), 5056–5071.

[12] Maresca, S., Braca, P., and Horstmann, J. Detection, tracking and fusion of multiple hfsw radars for ship traffic surveillance: experimental performance assessment. In *Proceedings of the IEEE International Geoscience and Remote Sensing Symposium* (IGARSS), Melbourne, Australia, July 2013.

[13] Maresca, S., Braca, P., and Horstmann, J. Data fusion performance of hfswr systems for ship traffic monitoring. In *Proceedings of International Conference on Information Fusion* (FUSION), July 2013.

[14] Maresca, S., Braca, P., Grasso, R., and Horstmann, J. Multiple oceanographic hf surface-wave radars applied to maritime surveillance. In

Proceedings of International Conference on Information Fusion (FUSION), July 2014.

[15] Maresca, S., Braca, P., Horstmann, J., and Grasso, R. A network of HF surface wave radars for maritime surveillance: preliminary results in the German Bight. In *Proceedings of IEEE International Conference on Acoustics, Speech and Signal Processing* (ICASSP), May 2014.

[16] Gurgel, K.-W., Essen, H.-H., and Kingsley, P. HF radars: physical limitations and recent developments. *Coastal Engineering,* Vol. 37, 3-4 (Aug. 1999), 201–218.

[17] Essen, H.-H., Gurgel, K.-W., and Schlick, T. On the accuracy of current measurements by means of HF radar. *IEEE Journal of Oceanic Engineering,* Vol. 25, 4 (Oct. 2000), 472–480.

[18] Gurgel, K.-W., Essen, H.-H., and Schlick, T. An empirical method to derive ocean waves from second-order Bragg scattering - prospects and limitations. *IEEE Journal of Oceanic Engineering,* Vol. 31, 4 (Oct. 2006), 804–811.

[19] Gurgel, K.-W., Dzvonkovskaya, A., Pohlmann, T., Schlick, T., and Gill, E. Simulation and detection of tsunami signatures in ocean surface currents measured by HF radar. *Ocean Dynamics,* Vol. 61, 10 (2011), 1495–1507.

[20] Skolnik, M. *Radar Handbook* (3rd ed.). NewYork: McGraw-Hill, 2008.

[21] Grosdidier, S., Baussard, A., and Khenchaf, A. HFSW radar model: simulation and measurement. *IEEE Transactions on Geoscience and Remote Sensing,* Vol. 48, 9 (Sept. 2010), 3539–3549.

[22] Maresca, S., Greco, M., Gini, F., Grasso, R., Coraluppi, S., and Thomas, N. The HF surface wave radar WERA. Part I: statistical analysis of recorded data. In *Proceedings of the IEEE Radar Conference,* Washington, DC, 2010.

[23] Maresca, S., Greco, M., Gini, F., Grasso, R., Coraluppi, S., and Thomas, N. The HF surface wave radar WERA. Part II: spectral analysis of recorded data. In *Proceedings of the IEEE Radar Conference,* Washington, DC, 2010.

[24] Riethmuller, R., Colijn, F., Krasermann, H., Schroeder, F., and Ziemer, F. Cosyna, an integrated coastal observation system for northern and arctic seas. In *Proceedings of the MTS/IEEE Oceans'09 Conference,* Oct. 2009.

[25] Pallotta, G., Horn, S., Braca, P., and Bryan, K. Context-enhanced vessel prediction based on Ornstein-Uhlenbeck processes using historical AIS traffic patterns: real-world experimental results. In *Proceedings of International Conference on Information Fusion* (FUSION), May 2014.

[26] Vivone, G., Braca, P., and Horstmann, J. Knowledge-based multi-target tracking via UKF-JPDA variable structure IMM estimator in HF surface wave radar systems. *IEEE Transactions on Geoscience and Remote Sensing,* to be published.

[27] Katsilieris, F., Braca, P., and Coraluppi, S. Detection of malicious AIS position spoofing by exploiting radar information. In *Proceedings of the* 16*th International Conference on Information Fusion* (FUSION 2013), July 2013.

[28] Julier, S. J., and Uhlmann, J. K. Unscented filtering and nonlinear estimation. *Proceedings of the IEEE,* Vol. 92, 3 (Mar. 2004), 401–422.

[29] Duan, Z., Li, X. R., Han, C., and Zhu, H. Sequential unscented Kalman filter for radar target tracking with range rate measurements. In *Proceedings of the* 8*th International Conference on Information Fusion* (FUSION), Philadelphia, PA, July 2005, 130–137.

[30] Bar-Shalom, Y. Negative correlation and optimal tracking with Doppler measurements. *IEEE Transactions on Aerospace and Electronic Systems,* Vol. 37, 3 (Aug. 2001), 1117–1120.

[31] Wan, E., and Van Der Merwe, R. The unscented Kalman filter for nonlinear estimation. In *Proceedings of Adaptive Systems for Signal Processing, Communications, and Control Symposium* (AS-SPCC), 2000, 153–158.

[32] Bruno, L., Braca, P., Horstmann, J., and Vespe, M. Experimental evaluation of the range-Doppler coupling on HF surface wave radars. *IEEE Geoscience and Remote Sensing Letters,* Vol. 10, 4 (2013), 850–854.

[33] Bar-Shalom, Y., Daum, F., and Huang, J. The probabilistic data association filter. *IEEE Control Systems Magazine,* Vol. 29, 6 (Dec. 2009), 82–100.

[34] Poore, A. B., Rijavec, N., Barker, T. N., and Munger, M. Data association problems posed as multidimensional assignment problems: problem formulation and numerical simulations. *Proceedings of SPIE,* vol. 1954, *Signal and Data Processing of Small Targets,* Apr. 1993, 552–573.

[35] Levedahl, M. Explicit pattern matching assignment algorithm. In *Proceedings of SPIE, Signal and Data Processing of Small Targets,* Aug. 2002.

[36] Kirubarajan, T., Bar-Shalom, Y., Pattipati, K. R., and Kadar, I. Ground target tracking with variable structure IMM estimator. *IEEE Transactions on Aerospace and Electronic Systems,* Vol. 36, 1 (July 2000), 26–46.

[37] Capraro, G., Farina, A., Griffiths, H., and Wicks, M. Knowledge-based radar signal and data processing: a tutorial review. *IEEE Signal Processing Magazine,* Vol. 23, 1 (Jan. 2006), 18–29.

[38] Horn, S., Arcieri, G., Millefiori, L., and Cimino, G. Information interoperability: lessons learned on interoperability standards in fusion and tracking. NATO-STO Centre for Maritime Research and Experimentation, Tech. Rep. CMRE-FR-2014-001, Feb. 2014 (NATO UNCLASSIFIED).

[39] Arcieri, G., Cimino, G., Horn, S., and Bryan, K. Web service interoperability in a network-enabled environment. NATO-STO Centre for Maritime Research and Experimentation, Tech. Rep. CMRE-FR-2014-003, Feb. 2014 (NATO UNCLASSIFIED).

[40] Cimino, G., Arcieri, G., Horn, S., and Bryan, K. Sensor data management to achieve information superiority in maritime situational awareness. NATO-STO Centre for Maritime Research and Experimentation, Tech. Rep. CMRE-FR-2014-017, Oct. 2014 (NATO UNCLASSIFIED).

[41] What is windows communication foundation. [Online]. Available: https://msdn.microsoft.com/en-us/library/ms731082(v=vs.110).aspx

[42] Vivone, G., Braca, P., and Horstmann, J. Variable structure interacting multiple model algorithm for ship tracking using HF surface wave radar data In *Proceedings of MTS/IEEE Oceans Conference,* May 2015, pp. 1–6.

[43] Vivone, G., Braca, P., and Horstmann, J. Knowledge-based ship tracking applied to HF surface wave radar data. In *Proceedings of the IEEE International Geoscience and Remote Sensing Sympsoium* (IGARSS), May 2015, 1–6.

[44] Koch, W., and Van Keuk, G. Multiple hypothesis track maintenance with possibly unresolved measurements. *IEEE Transactions on Aerospace and Electronic Systems,* Vol. 33, 3 (July 1997), 883–892.

[45] Blom, H., and Bloem, E. Bayesian tracking of two possibly unresolved maneuvering targets. *IEEE Transactions on Aerospace and Electronic Systems,* Vol. 43, 2 (Apr. 2007), 612–627.

[46] Granström, K., Natale, A., Braca, P., Ludeno, G., and Serafino, F. PHD extended target tracking using an incoherent X-band radar: preliminary real-world experimental results. In *Proceedings of the* 17*th International Conference on Information Fusion* (FUSION), Salamanca, Spain, July 2014.

[47] Granström, K., Natale, A., Braca, P., Ludeno, G., and Serafino, F. Gamma Gaussian inverse Wishart probability hypothesis density for extended target tracking using X-band marine radar data. *IEEE Transactions on Geoscience and Remote Sensing*, Vol. 53, 12 (2015), 6617–6631.

[48] Maresca, S., Braca, P., Grasso, R., Horstmann, J., and Seemann, J. Oceanographic HF surface-wave radars for maritime surveillance in the German Bight. In *Proceedings of OCEANS 2014 - TAIPEI,* Apr. 2014, 1–6.

[49] Papa, G., Braca, P., Horn, S., Marano, S., Matta, V., and Willett, P. Adaptive Bayesian tracking with unknown time-varying sensor network performance. In *Proceedings of 40th IEEE International Conference on Acoustics, Speech and Signal Processing* (ICASSP), Brisbane, Australia, 2015.

[50] Papa, G., Braca, P., Horn, S., Marano, S., Matta, V., and Willett, P. Multisensor adaptive Bayesian tracking under time-varying target detection capability. *IEEE Transactions on Aerospace and Electronic Systems,* submitted for publication.

[51] Meyer, F., Braca, P., Willett, P., and Hlawatsch, F. Scalable multitarget tracking using multiple sensors: a belief propagation approach. In *Proceedings of the* 18*th International Conference on Information Fusion* (FUSION), Washington, DC, 2015.

Document Data Sheet

Security Classification		Project No.
Document Serial No.	**Date of Issue**	**Total Pages**
CMRE-PR-2019-094	June 2019	15 pp.

Author(s)

Paolo Braca, Salvatore Maresca, Raffaele Grasso, Karna Bryan, Jochen Horstmann

Title

Maritime surveillance with multiple over-the-horizon HFSW radars: an overview of recent experimentation

Abstract

This paper briefly explores the high-frequency surface-wave (HFSW) radar technology in general, and Wellen radar (WERA) in more detail. Then it describes the multitarget tracking data fusion (MTTDF) network architecture developed at Science and Technology Organization (STO) Centre for Maritime Research and Experimentation (CMRE) and discusses its capabilities in two real study cases: the first in the Ligurian Sea, Mediterranean [11]-[13], and a second in the German Bight, North Sea [14], [15]. In both cases, the main task of the HFSW radars is to estimate sea surface currents. In the second study case, the data recorded by the single stations are sent directly to the Centre's Data Base (DB) and then processed in real-time. The historical information about ship traffic can be exploited not only for assessing system performance, but also in the field of knowledge-based (KB) tracking, for improving system capabilities. In this sense, simulation results are presented and discussed. Finally, a tool developed at STO CMRE, the so-called maritime situational awareness (MSA) viewer, allows displaying from the operator's point of view the maritime picture of the surveyed area.

Keywords

Surveillance, sea surface, marine vehicles, sea measurements, surface waves, Chirp modulation, radar measurements

Issuing Organization

NATO Science and Technology Organization
Centre for Maritime Research and Experimentation

Viale San Bartolomeo 400, 19126 La Spezia, Italy

[From N. America:
STO CMRE
Unit 31318, Box 19, APO AE 09613-1318]

Tel: +39 0187 527 361
Fax:+39 0187 527 700

E-mail: library@cmre.nato.int